nature COMMUNICATIONS

ARTICLE

Received 2 Feb 2012 | Accepted 10 Apr 2012 | Published 22 May 2012

DOI: 10.1038/ncomms1843

# Superionic glass-ceramic electrolytes for room-temperature rechargeable sodium batteries

Akitoshi Hayashi[1], Kousuke Noi[1], Atsushi Sakuda[1] & Masahiro Tatsumisago[1]

Innovative rechargeable batteries that can effectively store renewable energy, such as solar and wind power, urgently need to be developed to reduce greenhouse gas emissions. All-solid-state batteries with inorganic solid electrolytes and electrodes are promising power sources for a wide range of applications because of their safety, long-cycle lives and versatile geometries. Rechargeable sodium batteries are more suitable than lithium-ion batteries, because they use abundant and ubiquitous sodium sources. Solid electrolytes are critical for realizing all-solid-state sodium batteries. Here we show that stabilization of a high-temperature phase by crystallization from the glassy state dramatically enhances the $Na^+$ ion conductivity. An ambient temperature conductivity of over $10^{-4}$ S cm$^{-1}$ was obtained in a glass-ceramic electrolyte, in which a cubic $Na_3PS_4$ crystal with superionic conductivity was first realized. All-solid-state sodium batteries, with a powder-compressed $Na_3PS_4$ electrolyte, functioned as a rechargeable battery at room temperature.

[1] Department of Applied Chemistry, Faculty of Engineering, Osaka Prefecture University, Naka-ku, Sakai, Osaka 599-8531, Japan. Correspondence and requests for materials should be addressed to A.H. (email: hayashi@chem.osakafu-u.ac.jp).

Sodium-ion rechargeable batteries, using abundant sodium sources, are suitable for use in distributed power systems that store renewable energy at individual houses[1–4]. Currently, sodium – sulphur (NAS) batteries[5] are used for large-scale storage, because they have high energy densities of up to 760 Wh kg$^{-1}$. However, NAS batteries need to be operated at temperatures up to 300 °C to use liquid-state sulphur-positive electrodes and sodium-negative electrodes and to enhance the conductivity of β-alumina solid electrolyte, a well-known $Na^+$ ion conductor. From a safety viewpoint, NAS batteries that operate at room temperature are strongly desirable as they would be a suitable distributed storage for individual houses. All-solid-state batteries are the safest batteries, because they do not suffer from leakage, volatilization, or flammability, as they employ solid inorganic electrolytes rather than liquid organic electrolytes[6–8]. To realize solid-state batteries that operate at ambient and moderate temperatures, superior solid electrolytes that have high $Na^+$ ion conductivities at room temperature and close contact with electrode active materials are indispensable. Moreover, a drastic reduction in the interparticle resistance of electrolytes without high-temperature sintering is highly significant, because this is critical for developing large-scale solid-state batteries. However, no highly conductive electrolytes suitable for room-temperature operation of batteries have been found[9–15].

We have studied $Li^+$ ion conducting electrolytes and found that solid sulphide electrolytes made from the system $Li_2S$–$P_2S_5$ have a high conductivity and a wide electrochemical window[16,17], making them suitable for all-solid-state lithium secondary batteries that have excellent cycling and rate performances[18–21].

In this study, we developed a sulphide glass-ceramic electrolyte by crystallization of high-temperature cubic $Na_3PS_4$ phase from the glassy state. The prepared electrolyte showed a sodium-ion conductivity of $2\times10^{-4}$ S cm$^{-1}$ at room temperature. This high conductivity was achieved by stabilization of cubic $Na_3PS_4$ and large reduction of grain-boundaries in a glass-ceramic pellet. A room-temperature operation of all-solid-state rechargeable sodium batteries with a powder-compressed glass-ceramic electrolyte was first realized and this achievement is the first step toward realizing all-solid-state NAS batteries.

## Results

**Crystallization of $Na_3PS_4$ glass electrolytes**. Ortho-thiophosphate $Na_3PS_4$ glass was prepared by a mechanochemical technique using a planetary ball mill; the synthesized sample exhibited a halo pattern in its X-ray diffraction (XRD) pattern (Fig. 1a) and a glass transition at 180 °C in differential thermal analysis (DTA, Fig. 1d). A Raman spectrum of the glass (Fig. 1e) revealed that the glass had a single band at 420 cm$^{-1}$, which is attributable to the ortho-thiophosphate ion ($PS_4^{3-}$) (ref. 22). This implies that the glass had the nominal composition.

As shown in Fig. 1b, a crystalline phase was precipitated after heating the $Na_3PS_4$ glass at 270 °C, which is above the first crystallization temperature determined by DTA. The XRD pattern of the glass-ceramic (that is, crystallized glass) was indexed by a cubic phase based on a tetragonal phase of $Na_3PS_4$ (JCPDS #081-1472). Cubic $Na_3PS_4$ is considered to be a high-temperature phase of tetragonal $Na_3PS_4$ (ref. 12), but the cubic phase of $Na_3PS_4$ has not been reported previously. The glass-ceramic obtained by heating at a higher temperature of 420 °C had a different XRD pattern that is attributable to the low-temperature phase of tetragonal $Na_3PS_4$ (ref. 12) (Fig. 1c).

**Electrical conductivity of $Na_3PS_4$ solid electrolytes**. A powder-compressed pellet of the $Na_3PS_4$ glass and the glass-ceramic pellet prepared at 270 °C with carbon electrodes on both surfaces were evaluated by alternating current impedance measurements. Figure 2a shows impedance plots of the pellets. The impedance plots of the glass pellet exhibit a semicircle and a spike in the low-frequency region, suggesting that the glass behaves as a typical ionic conductor. The total conductivity, which includes the bulk-grain and grain-boundary resistances, was determined from the cross-sectional resistance between the semicircle and the spike on the *x* axis. In contrast, impedance plots of the pellet of the glass-ceramic with the cubic $Na_3PS_4$ phase exhibits only a spike and the resistance of the pellet decreases by a factor of 30 on crystallization.

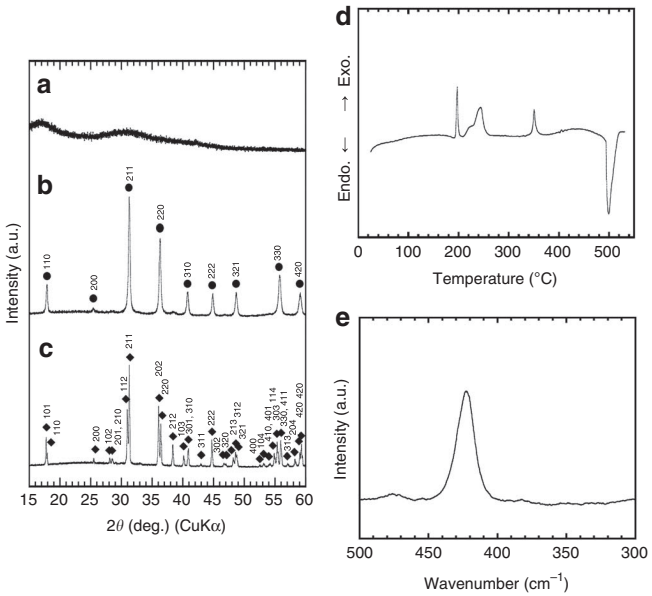


**Figure 1 | Characterization of the $Na_3PS_4$ glass and glass-ceramic electrolytes.** (**a**,**b**,**c**) XRD patterns of the $Na_3PS_4$ glass (**a**), glass-ceramic sample heated at 270 °C (**b**), and glass-ceramic sample heated at 420° C (**c**). Closed circles and diamonds, respectively, denote the diffraction peaks attributable to the cubic $Na_3PS_4$ phase and the tetragonal $Na_3PS_4$ phase (JCPDS #081-1472). (**d**) DTA curve of the $Na_3PS_4$ glass. (**e**) Raman spectrum of the $Na_3PS_4$ glass.

The conductivities of the $Na_3PS_4$ glass and glass-ceramic were compared with the conductivity of β-alumina as a typical $Na^+$ ion conductor. A pellet of β-alumina was prepared by cold-pressing its powders, which had been sufficiently pulverized, and its impedance was measured as a function of frequency. Figure 2b shows Bode plots of the electrolyte pellets of the $Na_3PS_4$ glass (25 °C), the glass-ceramic (25 °C), and β-alumina (70 and 120 °C). (The data for the glass and glass-ceramic are the same as those shown in Fig. 2a). The absolute values of impedance $|Z|$ as a function of frequency of β-alumina behave completely differently from those of the $Na_3PS_4$ glass and glass-ceramic. The glass-ceramic has smaller impedance than β-alumina in the high-frequency range from $10^4$ to $10^7$ Hz, whereas the impedance of β-alumina at 70 °C is six orders of magnitude larger than that of glass-ceramic at low frequencies in the range 0.1 to 10 Hz. This is clear evidence that the $Na_3PS_4$ glass-ceramic pellet possesses a higher ionic motion than the β-alumina pellet. Cross-section of the pellets was analysed by scanning electron microscope (SEM). Grain-boundaries among particles are clearly observed in the β-alumina pellet (Fig. 2d), whereas intimate contacts among particles are achieved in the $Na_3PS_4$ glass-ceramic pellet (Fig. 2c). The difference in microstructure affects the total conductivity (especially conductivity at grain-boundary) of the pellets.

Figure 3 shows the electrical conductivities of $Na_3PS_4$ glass, glass-ceramic electrolytes, and typical inorganic solid electrolytes[9–15] that have $Na^+$ ion conductivities. All the conductivities in this figure were determined from the total resistance, which includes both bulk-grain and grain-boundary components. The $Na_3PS_4$ glass pellet (open circles) has a conductivity of $6\times10^{-6}$ S cm$^{-1}$ at room

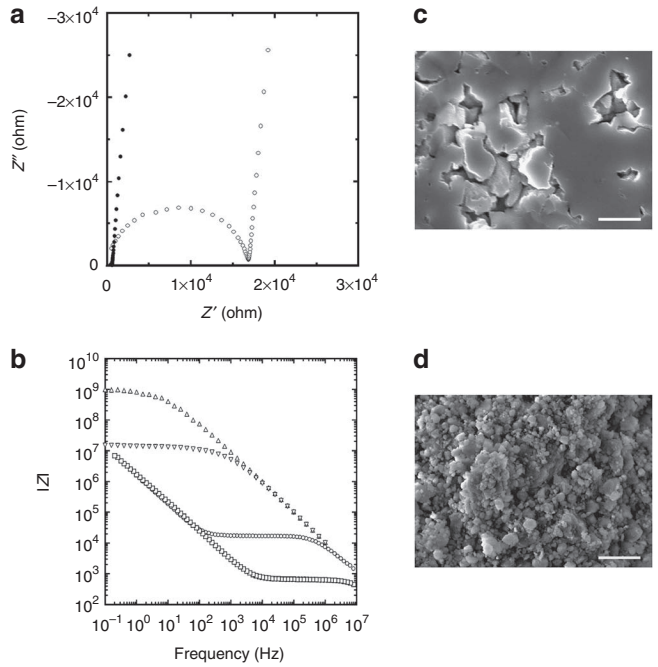


**Figure 2 | Impedance and morphology of the $Na_3PS_4$ glass, the $Na_3PS_4$ glass-ceramic and β-alumina electrolytes.** (**a**) Impedance plots at 25 °C of a powder-compressed pellet of the $Na_3PS_4$ glass (open circle) and the glass-ceramic pellet prepared at 270 °C (closed circle). (**b**) Bode plots of the pellets of the $Na_3PS_4$ glass (open circle, at 25 °C) and the $Na_3PS_4$ glass-ceramic (open square, at 25 °C), and the β-alumina (open triangle (at 70 °C) and open reverse-triangle (at 120 °C)). (**c**,**d**) Cross-sectional SEM images of the $Na_3PS_4$ glass-ceramic pellet (**c**) and the β-alumina pellet (**d**). Scale bar, 5 μm.

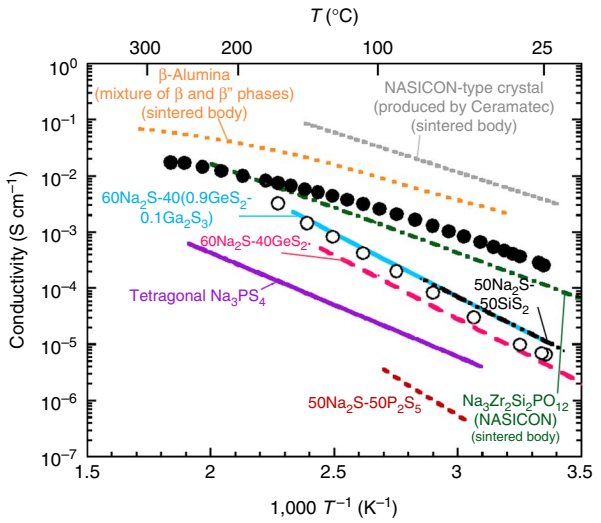


**Figure 3 | Conductivity of the $Na_3PS_4$ glass and glass-ceramic electrolytes.** Temperature dependences of the conductivities of the $Na_3PS_4$ glass (open circles) and the glass-ceramic prepared at 270 °C (solid circles). Conductivities of several $Na^+$ ion conductors reported so far are also shown as a comparison.

temperature and an activation energy for conduction of 47 kJ mol$^{-1}$; it has similar conductivity properties to those of sulphide glasses in systems such as $Na_2S$–$SiS_2$ and $Na_2S$–$GeS_2$ (refs 9–11. On the other hand, the glass-ceramic with cubic $Na_3PS_4$ (closed circles) has a conductivity of $2\times10^{-4}$ S cm$^{-1}$ at room temperature and an activation energy of 27 kJ mol$^{-1}$. The presence of cubic $Na_3PS_4$ is responsible for the large increase in the conductivity of the glass-ceramic electrolyte because tetragonal $Na_3PS_4$, which is the low-temperature phase, has a conductivity of $1\times10^{-6}$ S cm$^{-1}$ at room temperature[12]. The $Na_3PS_4$ glass-ceramic electrolyte has a higher conductivity than sulphide glasses[9–11] and a $Na_3Zr_2Si_2PO_{12}$ NASICON crystal[14]. Several sintered electrolytes such as β-alumina (consisting of β and β″ phases)[13] and a NASICON-type crystal (produced by Ceramatec)[15] have a higher conductivity of $10^{-3}$ S cm$^{-1}$ at room temperature; sintering at a high temperature of 1,800 °C is needed to reduce the grain-boundary resistance for β-alumina[13]. Although the conductivity of the $Na_3PS_4$ glass-ceramic electrolyte is one order of magnitude lower than that of sintered β-alumina and the NASICON-type crystal, the use of the sulphide glass-ceramic results in good electrode–electrolyte contact by simple cold pressing.

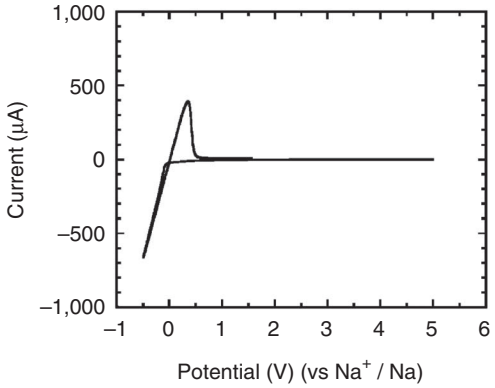


**Figure 4 | Cyclic voltammogram of the $Na_3PS_4$ glass-ceramic electrolyte.** The glass-ceramic was prepared at 270 °C. A stainless-steel disk, as the working electrode, and a sodium foil, as the counter/reference electrode, were used. The potential sweep was performed with a scanning rate of 5 mV s$^{-1}$ at 25 °C.

**Application to all-solid-state sodium batteries**. The electrochemical window of the sulphide glass-ceramic electrolyte with cubic $Na_3PS_4$ was examined by performing cyclic voltammetry measurements. As shown in Fig. 4, reversible sodium deposition and dissolution currents were observed at about 0 V versus $Na^+$/Na, and no remarkable oxidation currents were observed up to 5 V. This suggests that the sulphide electrolyte has a wide electrochemical window of 5 V and is electrochemically stable against Na metal.

All-solid-state test cells were fabricated using the $Na_3PS_4$ glass-ceramic solid electrolyte. A three-layered pellet of Na–Sn alloy (counter and reference electrodes)/$Na_3PS_4$ (solid electrolyte)/$TiS_2$ (working electrode) was prepared by cold pressing at room temperature. The $TiS_2$ electrode was selected as a model active material in $Na^+$ ion batteries, because of its large electronic conductivity and good electrochemical performance in organic liquid electrolyte cells[23]. Figure 5 shows charge–discharge curves of the all-solid-state cell (Na–Sn/$Na_3PS_4$/$TiS_2$) at room temperature. The cell operated as a rechargeable sodium battery at room temperature. The average cell voltages from the second to tenth cycles were 1.6 V, which approximately correspond to the potential difference between the Na–Sn counter electrode (ca. 0.3 V versus $Na^+$/Na)[24] and the $TiS_2$ working electrode (ca. 2.0 V versus $Na^+$/Na)[23]. The reversible capacity of the cell was about 90 mAh per gram of $TiS_2$ and the cell kept the capacity for 10 cycles. This is the first case that room-temperature operation of all-solid-state rechargeable sodium batteries using inorganic electrolyte powders has been reported.

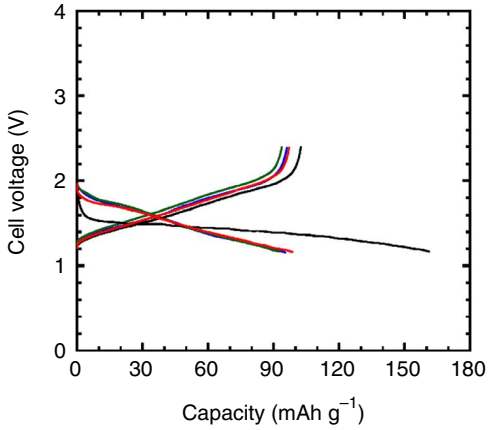


**Figure 5 | Charge-discharge curves of the all-solid-state rechargeable sodium cell Na-Sn / $Na_3PS_4$ glass-ceramic / $TiS_2$.** The black, red, blue and green lines, respectively, denote the first, second, third and tenth cycles. The cell operation was carried out at 25 °C at the current density of 0.013 mA cm$^{-2}$.

## Discussion

A high conductivity of the $Na_3PS_4$ glass-ceramic electrolyte is originally from the precipitation of the cubic $Na_3PS_4$ phase from the glassy state. A high-temperature phase, such as α-AgI ($Ag^+$ superionic conductor)[25,26] or $Li_7P_3S_{11}$ ($Li^+$ superionic conductor)[16,17], with a high ionic conductivity precipitates as the first crystal from a supercooled liquid above the glass transition temperature. This is the first time for sodium ion conductors that cubic $Na_3PS_4$ has been stabilized as a high-temperature phase. The cubic $Na_3PS_4$ phase was at least stable even after storage for half-a-year at room temperature in an Ar-filled glove box. A glass component does not completely vanish by crystallization, and thus the remaining glass part would have an important role in stabilizing a high-temperature phase, cubic $Na_3PS_4$. Detailed analysis of the glass component in the glass-ceramic electrolyte is now in progress.

Oxide $Na^+$ ion conductors including β-alumina generally require high-temperature sintering to reduce their grain-boundary resistance; this sintering may deteriorate the electrode–electrolyte interface through undesirable side reactions. Therefore, the low grain-boundary resistance of the $Na_3PS_4$ glass-ceramic pellet is highly advantageous for achieving good electrode–electrolyte contact in all-solid-state batteries.

All-solid-state rechargeable sodium cells (Na–Sn/$TiS_2$) with a powder-compressed $Na_3PS_4$ glass-ceramic electrolyte functioned at room temperature. Although the capacity was limited to nearly 40% of the theoretical capacity of $TiS_2$, the all-solid-state cell has the potential to realize good charge–discharge reversibility. Utilization of active materials and rate performance would be enhanced by optimizing preparation technique of composite positive electrodes[27,28] and increasing conductivity of solid electrolytes by their structural modification[17,18,29], which are based on our experimental results found in all-solid-state lithium secondary batteries. Work to improve the battery performance is currently in progress. The findings presented here represent the first step towards realizing practical all-solid-state $Na^+$ ion batteries that are safe and inexpensive. We have reported excellent cycle performance of all-solid-state lithium-sulphur batteries at room temperature by formation of intimate contact among sulphur, a glass-ceramic electrolyte and a conductive additive, using a ball-milling technique[30,31]. We thus believe that all-solid-state NAS batteries, which operate at room temperature, will be developed in the near future. Such next-generation batteries contribute to the realization of a low-carbon society by efficient use of sustainable energy.

## Methods

**Preparation $Na_3PS_4$ glass and glass-ceramic electrolytes**. $Na_3PS_4$ glass was prepared by a mechanochemical technique using a planetary ball mill (Fritsch, Pulverisette 7). The starting materials of 75 mol% $Na_2S$ (Aldrich) and 25 mol% $P_2S_5$ (Aldrich) were hand-ground and the mixture was then placed into a zirconia ($ZrO_2$) vessel (internal volume of 45 ml) with 500 $ZrO_2$ balls (4 mm in diameter). The mechanochemical reaction was performed for 20 h at a fixed rotation speed of the base disc of 510 r.p.m. to form $Na_3PS_4$ glass powders. The contamination from the vessel and ball media was analysed by inductively coupled plasma atomic emission spectroscopy (ICP-AES; Seiko Instruments, SPS7800); the amount of $ZrO_2$ estimated from the amount of Zr in the milled $Na_3PS_4$ glass was ca 0.1 wt%, and, thus, the trace amount of $ZrO_2$ would not affect conductivity and crystal phase of glass-ceramics. The glass powder was compressed by a conventional uniaxial cold press to prepare a pellet that was 10 mm in diameter and 1–1.5 mm thick. In the $Na_3PS_4$ glass, several crystallization peaks were observed at 200–260 °C and at about 350 °C in the DTA curve (Fig. 1d), and different crystal phases were precipitated over those crystallization temperatures. To obtain glass-ceramics with different crystals, the glass pellets were crystallized by heating at 270 or 420 °C, in an electric furnace, for 2 h. All the processes were performed in a dry Ar atmosphere.

**Characterization of solid electrolytes**. XRD (MAC Science, M18XHF$^{22}$-SRA) measurements of the prepared materials were performed using Cu Kα to identify the crystalline phases. Raman spectra of the glass were obtained using a Raman spectrophotometer (Jasco, NR-1000), using the 514 nm line of an Ar laser. DTA was performed by using a thermal analyser (Rigaku, Thermo Plus TG8110) at a heating rate of 10 °C min$^{-1}$. Microstructure of cross-section for the electrolyte pellets was observed by SEM (JEOL, JSM-6610A). The ionic conductivities of the pelletized samples were measured. Carbon paste was painted to form electrodes on both faces of the pellets. Two stainless-steel discs coupled with Pt wires were attached to the pellets as a current collector. Alternating current impedance measurements were performed for the obtained two-electrode cell in a dry Ar gas atmosphere, using an impedance analyser (Solartron, 1260) in the frequency range of 0.1 Hz to 8 MHz. Cyclic voltammetry measurements were conducted to investigate the electrochemical properties of the solid electrolytes. A stainless-steel disk as the working electrode and a sodium foil as the counter electrode were attached to each face of the pellet. The potential sweep was performed by using a potentiostat/galvanostat device (Hokuto Denko, HSV-100) with a scanning rate of 5 mV s$^{-1}$ at room temperature.

**Evaluation of all-solid-state sodium batteries**. An all-solid-state test cell was fabricated using $TiS_2$ as the working electrode, $Na_3PS_4$ glass-ceramic as the solid electrolyte, and a Na–Sn alloy as the counter and reference electrodes. The working electrode was a composite of $TiS_2$ active material and the solid electrolyte powders, because sodium ion paths to the active material are required to operate the cell. A reagent-grade $TiS_2$ (Kojundo Chemical Laboratory) and the $Na_3PS_4$ glass-ceramic with the weight ratio of 2:3 were well-mixed using an agate mortar and pestle. The working electrode (10 mg) and the solid electrolyte (80 mg) powders were placed in a 10-mm-diameter polycarbonate tube and pressed together by applying a pressure of 360 MPa. A Na foil (*ca* 90 μm) and Sn foil (15 μm), where the molar ratio of Na to Sn was almost 3, was then placed on the surface of the solid electrolyte side of the bilayer pellet and a pressure of 120 MPa was applied to the three-layered pellet. The three-layered pellet was sandwiched between two stainless-steel rods as current collectors. All the cell preparation processes were performed in a dry Ar-filled glove box. Electrochemical tests were conducted at a constant current density of 0.013 mA cm$^{-2}$ (ca 0.01 C) in the voltage range from 1.17 to 2.40 V at room temperature under an Ar atmosphere using a charge–discharge measurement device (Nagano, BTS-2004).

## References

1. Delmas, C., Braconnier, J. J, Fouassier, C. & Hagenmuller, P. Electrochemical intercalation of sodium in $Na_xCoO_2$ bronzes. *Solid State Ionics* **3-4,** 165–169 (1981).
2. Komaba, S., Takei, C., Nakayama, T., Ogata, A. & Yabuuchi, N. Electrochemical intercalation activity of layered $NaCrO_2$ versus $LiCrO_2$. *Electrochem. Commun.* **12,** 355–358 (2010).
3. Nishijima, M., Gocheva, I. D., Okada, S., Doi, T., Yamaki, J. I. & Nishida, T. Cathode properties of metal trifluorides in Li and Na secondary batteries. *J. Power Sources* **190,** 558–562 (2009).
4. Park, C. W., Ryu, H. S., Kim, K. W., Ahn, J.- H., Lee, J. Y. & Ahn, H. J. Discharge properties of all-solid sodium-sulfur battery using poly (ethylene oxide) electrolyte. *J. Power Sources* **165,** 450–454 (2007).
5. Lu, X., Xia, G., Lemmon, J. P & Yang, Z. Advanced materials for sodium-beta alumina batteries: status, challenges and perspectives. *J. Power Sources* **195,** 2431–2422 (2010).

6. Armand, M. & Tarascon, J.- M. Building better batteries. *Nature* **451,** 652–657 (2008).
7. Tarascon, J.- M. & Armand, M. Issues and challenges facing rechargeable lithium batteries. *Nature,* **414,** 359–367 (2001).
8. Kamaya, N. & , *et al.* A lithium superionic conductor. *Nat. Mater.* **10,** 682–686 (2011).
9. Ribes, M., Barrau, B. & Souquet, J. L. Sulfide glasses: glass forming region, structure and ionic conduction of glasses in $Na_2S$-$XS_2$ (X=Si; Ge), $Na_2S$-$P_2S_5$ and $Li_2S$-$GeS_2$ systems. *J. Non-Cryst. Solids* **38&39,** 271–276 (1980).
10. Susman, S., Boehm, L., Volin, K. J. & Delbecq, C. J. A new method for the preparation of fast-conducting, reactive glass systems. *Solid State Ionics* **5,** 667–670 (1981).
11. Yao, W. & Martin,, S. W. Ionic conductivity of glasses in the MI+$M_2S$+(0.1 $Ga_2S_3$+0.9$GeS_2$) system (M=Li, Na, K and Cs). *Solid State Ionics* **178,** 1777–1784 (2008).
12. Jansen, M. & Henseler, U. Synthesis, structure determination, and ionic conductivity of sodium tetrathiophoshate. *J. Solid State Chem.* **99,** 110–119 (1992).
13. Hooper, A. A study of the electrical properties of single-crystal and polycrystalline β-alumina using complex plane analysis. *J. Phys. D: Appl. Phys.,* **10,** 1487–1496 (1977).
14. Bohnke, O., Ronchetti, S. & Mazza, D. Conductivity measurements on nasicon and nasicon-modified materials. *Solid State Ionics* **122,** 127–136 (1999).
15. Coors, W. G., Gordon, J. H. & Menzer, S. G. Electrochemical cell comprising ionically conductive membrane and porous multiphase electrode. *US patent* US2010/0297537A1 (2010).
16. Mizuno, F., Hayashi, A., Tadanaga, K. & Tatsumisago, M. New, highly ion-conductive crystals precipitated from $Li_2S$-$P_2S_5$ glasses. *Adv. Mater.* **17,** 918–921 (2005).
17. Hayashi, A., Miami, K., Ujiie, S. & Tatsumisago, M. Preparation and ionic conductivity of $Li_7P_3S_{11-z}$ glass-ceramic electrolytes. *J. Non-Cryst. Solids* **356,** 2670–2673 (2010).
18. Minami, T., Hayashi, A. & Tatsumisago, M. Recent progress of glass and glass-ceramics as solid electrolytes for lithium secondary batteries. *Solid State Ionics* **177,** 2715–2720 (2006).
19. Ohta, N., Takada, K., Zhang, L., Ma, R., Osada, M. & Sasaki, T. Enhancement of the high-rate capability of solid-state lithium batteries by nanoscale interfacial modification. *Adv. Mater.* **18,** 2226–2229 (2006).
20. Tatsumsiago, M. & Hayashi, A. All-solid-state lithium secondary batteries using sulfide-based glass ceramic electrolytes. *Funct. Mater. Lett.* **1,** 31–36 (2008).
21. Sakuda, A., Hayashi, A. & Tatsumisago, M. Interfacial observation between $LiCoO_2$ electrode and $Li_2S$-$P_2S_5$ solid electrolytes of all-solid-state lithium secondary batteries using transmission electron microscopy. *Chem. Mater.* **22,** 949–956 (2010).
22. Tachez, M., Malugani, J. P., Mercier, R. & Robert, G. Ionic conductivity and phase transition in lithium thiophosphate $Li_3PS_4$. *Solid State Ionics* **14,** 181–185 (1984).
23. Whittingham, M. S. Chemistry of intercalation compounds: metal guests in chalcogenide hosts. *Prog. Solid State Chem.* **12,** 41–99 (1978).
24. Inoue, T., Kanai, K., Itaya, M. & Fujimoto, M. Negative electrode and non-aqueous electrolyte secondary battery with it (in Japanese). *JP Patent* 2006-244976 (2006).
25. Tatsumisago, M., Shinkuma, Y. & Minami, T. Stabilization of superionic α-AgI at room temperature in a glass matrix. *Nature* **354,** 217–218 (1991).
26. Tatsumsiago, M., Saito, T. & Minami, T. Stabilization of superionic α-AgI at room temperature by heating of AgI-$Ag_2O$-$MoO_3$ glasses. *Chem. Lett.* 790–791 (2001).
27. Mizuno, F., Hayashi, A., Tadanaga, K. & Tatsumisago, M. Effects of conductive additives in composite positive electrodes on charge-discharge behaviors of all-solid-state lithium secondary batteries. *J. Electrochem. Soc.* **152,** A1499–A1503 (2005).
28. Kitaura, H., Hayashi, A., Ohtomo, T., Hama, S. & Tatsumisago, M. Fabrication of electrode-electrolyte interfaces in all-solid-state rechargeable lithium batteries by using a supercooled liquid state of the glassy electrolytes. *J. Mater. Chem.* **21,** 118–124 (2011).
29. Minami, K., Hayashi, A., Ujiie, S. & Tatsumisago, M. Electrical and electrochemical properties of glass-ceramic electrolytes in the systems $Li_2S$-$P_2S_5$-$P_2S_3$ and $Li_2S$-$P_2S_5$-$P_2O_5$. *Solid State Ionics* **192,** 122–125 (2011).
30. Hayashi, A., Ohtomo, T., Mizuno, F., Tadanaga, K. & Tatsumisago, M. All-solid-state Li/S batteries with highly conductive glass-ceramic electrolytes. *Electrochem. Commun.* **5,** 701–705 (2003).
31. Nagao, M., Hayashi, A. & Tatsumisago, M. Sulfur-carbon composite electrode for all-solid-state Li/S battery with $Li_2S$-$P_2S_5$ solid electrolyte. *Electrochim. Acta* **56,** 6055–6059 (2011).


## Acknowledgements

This research was supported by JST, 'Advanced Low Carbon Technology Research and Development Program (ALCA)'.

## Author Contributions

K.N. performed the synthesis and characterization of materials. A.S. contributed to impedance analysis. A.H. and M.T. designed the study, analysed the data and wrote the paper.

## Additional information

**Competing financial interests:** The authors declare no competing financial interests.



**How to cite this article:** Hayashi, A. *et al.* Superionic glass-ceramic electrolytes for room-temperature rechargeable sodium batteries. *Nat. Commun.* 3:856 doi: 10.1038/ncomms1843 (2012).